

Forecasting global aluminium flows to demonstrate the need for improved sorting and recycling methods

Peer-reviewed author version

Van den Eynde , S; Bracquene, E; Diaz-Romero, D; Zaplana, I; ENGELEN, Bart; Duflou, JR & Peeters, Jef (2022) Forecasting global aluminium flows to demonstrate the need for improved sorting and recycling methods. In: Waste management (Elmsford), 137 , p. 231 -240.

DOI: 10.1016/j.wasman.2021.11.019

Handle: <http://hdl.handle.net/1942/37730>

Forecasting Global Aluminium Flows to Demonstrate the Need for Improved Sorting and Recycling Methods

Simon Van den Eynde¹, Ellen Bracquené¹, Dillam Diaz-Romero^{1,2}, Isiah Zaplana¹, Bart Engelen^{1,3}, Joost R. Duflou^{1,4}, Jef R. Peeters¹

Department of Mechanical Engineering - KU Leuven, Celestijnenlaan 300A, Box 2422, 3001 Leuven, Belgium¹

PSI-EAWISE - KU Leuven, 2860 Sint-Katelijne-Waver, Belgium²

Technology Campus Diepenbeek - KU Leuven, Agoralaan Gebouw B, 3590 Diepenbeek, Belgium³

Member of Flanders Make⁴

Abstract

The probable emergence of a global aluminium scrap surplus in the coming decade is one of the main incentives for the aluminium recycling industry to invest in new methods and technologies to collect, sort and recycle aluminium scrap. However, due to the considerable uncertainty in the evolution of the global scrap surplus, it is difficult for policymakers and the recycling industry to accurately estimate the economic and environmental advantages of implementing enhanced sorting and recycling methods. The International Aluminium Institute (IAI) has developed a model to track and forecast the global flows of aluminium, but this model is not extensive enough to estimate the scrap surplus evolution. Therefore, this paper introduces an alloy series resolution to the supply and demand of aluminium in the IAI's global flow model and estimates the composition of the recovered scrap flows to improve the estimate of the technical potential of secondary alloy production. The estimated scrap surplus evolution is subjected to a sensitivity analysis, considering the most critical parameters, including the speed of electrification in the automotive sector, the recovered scrap's composition and the lifetime of aluminium products. In addition, the estimated

28 composition of the recovered aluminium scrap in the model is compared to composition
29 measurements of aluminium scrap collected at a Belgian recycling facility as a means of
30 validation. This study allows to estimate that the global aluminium scrap surplus will emerge
31 soon and reach a size of 5.4 million tonnes by 2030 and 8.7 million tonnes by 2040, if
32 currently adopted aluminium sorting and recycling methods are not improved.

33 **Keywords:** *Aluminium, Forecasting, Material Flow Analysis, Alloys, Scrap surplus*

34 1 Introduction

35 The demand for aluminium has been increasing drastically since 1950 due to the global
36 population's growth and the improved standard of living (European Aluminium Association,
37 2021). To date, aluminium is the second most-produced metal, preceded only by steel.
38 Aluminium is produced more than all other non-ferrous metals combined (Cullen and
39 Allwood, 2013). In the last two decades, the demand for aluminium has grown faster than
40 that for any other metal, increasing at a significantly faster rate than the global GDP (Fog,
41 2019). Its light weight, high strength, good corrosion resistance and high conductivity make
42 aluminium an attractive choice for many products, including food packaging, car parts,
43 airplane components and building features. The increased use of aluminium has led to
44 significant weight reductions of components in the automotive and aerospace sector which
45 have saved large amounts of fuel in the use phase of cars, trucks, and planes (European
46 Aluminium Association, 2013). However, aluminium production itself has substantial
47 environmental impact, in the form of toxicity, acidification, greenhouse gas emissions and
48 resource depletion (Schlesinger, 2017; The Economist, 2007). In 2020, the primary
49 production of aluminium was responsible for the emission of more than 1 billion metric
50 tonnes of CO₂-equivalents, accounting for almost 2% of the global human-caused emissions
51 in that year (Saevarsdottir et al., 2020; Van Heusden et al., 2020). In order to reduce the
52 aluminium industry's environmental impact, companies and policymakers increasingly focus

53 on aluminium recycling as a potential solution, with as main driver the substantial difference
54 in energy consumption: producing 1 kg of recycled aluminium requires on average 9.2 MJ,
55 compared to 144.6 MJ for producing 1 kg of primary aluminium (Peng et al., 2019).

56 The European Aluminium Association (EAA), the organisation representing the European
57 aluminium industry, forecasts a rise in the share of recycled aluminium in European end-use
58 products from 26% in 2000 to 49% in 2050 (European Aluminium Association, 2019). In its
59 “VISION 2050” report, the EAA explains that this is an ambitious but realistic evolution that
60 will significantly contribute to the European decarbonisation efforts. However, most collected
61 aluminium scrap today contains a mixture of different alloy types. As a result, different
62 alloying elements and impurities are present in the scrap. Removing these elements
63 metallurgically from the secondary aluminium is notoriously difficult (Nakajima et al., 2010).
64 Therefore, most collected aluminium scrap is “downcycled” and used for the production of
65 cast aluminium alloys, which have high tolerances for impurities (Paraskevas et al., 2015). A
66 smaller share of the collected scrap is used to produce wrought aluminium alloys, which have
67 much lower tolerances for alloying elements and impurities. To produce wrought alloys from
68 mixed scrap, it needs to be diluted with large amounts of primary aluminium.

69 Although this downcycling practice has been a successful strategy because of the high
70 demand for cast aluminium alloys for the production of combustion engines, this is expected
71 to change with the electrification of the automotive industry. Due to this transition, the global
72 demand for cast aluminium alloys will stagnate or is even expected to decline
73 (BloombergNEF, 2019; Modaresi and Müller, 2012). Simultaneously, the amount of
74 aluminium scrap collected from end-of-life products and the demand for wrought aluminium
75 alloys will keep growing. Previous research has suggested that, if the current practice of
76 systematic downcycling is maintained, the collected amount of aluminium scrap will soon
77 exceed the capacity of wrought and cast alloy production to absorb the secondary aluminium.

78 As such, an amount of aluminium scrap would be collected for which there is no suitable
79 application. This amount of aluminium scrap is commonly referred to as a scrap surplus.
80 Hatayama et al. (2012) estimate the scrap surplus size at 6.1 million tonnes in 2030. Modaresi
81 and Müller (2012) and Modaresi et al. (2014) expect a scrap surplus of 4.2 million tonnes in
82 2030 that will grow to a size of 14 million tonnes by 2050. However, they add that due to the
83 uncertainty in their parameters, the scrap surplus's actual size could lie anywhere between 3.3
84 and 18.3 million tonnes in 2050.

85 Therefore, this paper estimates the evolution of the global scrap surplus by expanding the
86 global flow model of the International Aluminium Institute (IAI). This model is a prominent
87 tool in the aluminium industry that tracks and predicts the volumes of aluminium throughout
88 the different life cycle stages. In this paper, an alloy series resolution is introduced in the
89 supply and demand data of the IAI and the composition of the recovered scrap flows is
90 estimated to improve the estimate of the technical potential of secondary alloy production.
91 The estimated evolution of the global scrap surplus is also subjected to a sensitivity analysis,
92 considering the most critical uncertain parameters that affect its growth. In addition, the
93 estimated composition of the recovered aluminium scrap in the model is compared to
94 composition measurements of aluminium scrap collected at a Belgian recycling facility as a
95 means of validation. These measurements are performed using a handheld X-Ray
96 Fluorescence (XRF) device.

97 2 Methodology

98 2.1 Demand for Aluminium Alloys

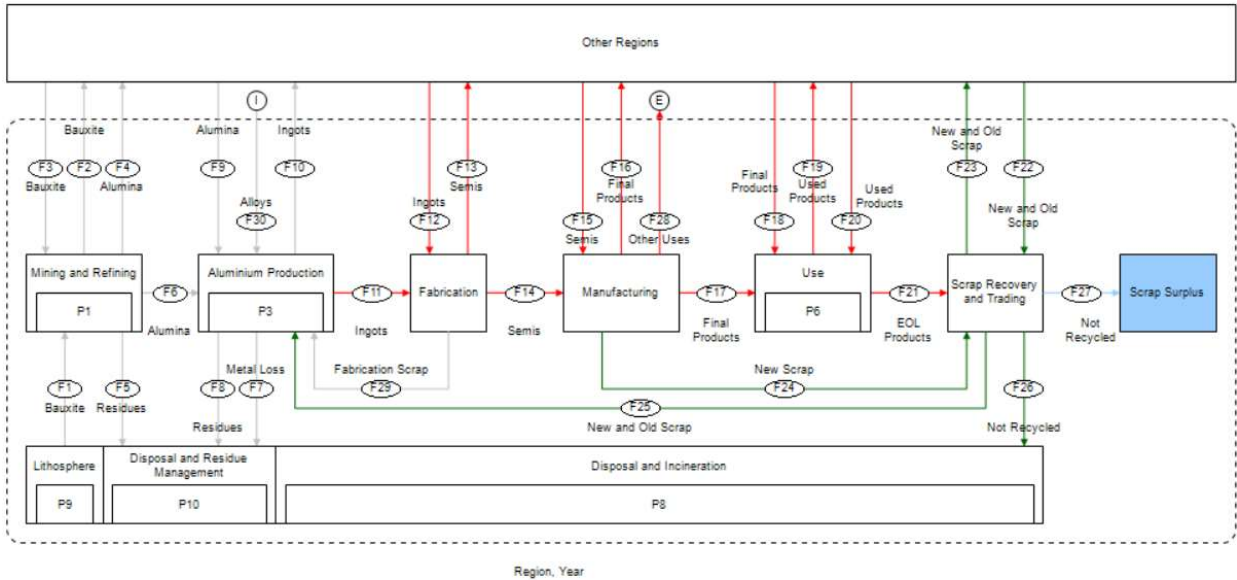
99 The IAI publishes annual data on the global flows of aluminium from different studies and
100 surveys. Bertram et al. (2009) combined these data into a single model, which resulted in the
101 first global flow model for aluminium, published in 2009. Ever since, the global aluminium

102 flow model of the IAI has been updated regularly (Bertram et al., 2017). Stakeholders in the
103 aluminium industry often refer to the model, that is freely accessible on the website of the IAI
104 (NTNU et al., 2020). Similar efforts to model and predict (global) flows of aluminium have
105 been made by other researchers as well (Dai et al., 2019; Zhu et al., 2021).

106 Figure 2.1 is adapted from Bertram et al. (2017) and shows the structure of the IAI's global
107 flow model. It models the flows of aluminium throughout the life cycle stages per region and
108 then links all regions together. The global flow data of the IAI include the amounts of
109 aluminium that flow to the manufacturing phase in the different industrial sectors since 1950,
110 and projections are made for these flows until the year 2040. Because the IAI has access to
111 extensive databases from reliable sources worldwide, the accuracy of their data is
112 unparalleled. No other material industry has succeeded in quantitatively modelling global
113 material flows with a similar level of accuracy (Bertram et al., 2009). However, the major
114 drawback of the MFA model of the IAI is that the aluminium is treated as a single, uniform
115 material that seems unaltered when it goes from one stage in the lifecycle to the next.

116 However, in practice aluminium is mostly alloyed, and the aluminium material flows undergo
117 significant compositional changes, especially in the end-of-life phase. Another significant
118 drawback of the IAI's model is that it assumes that all collected aluminium scrap can be
119 remelted into new alloys without verifying the allowable recycled content. Therefore, the
120 IAI's model cannot predict a possible emergence of a scrap surplus. Furthermore, the authors
121 chose to rely on projections of the EAA (European Aluminium Association, 2019) for the
122 demand for aluminium between 2030 and 2040 instead of using the numbers of the IAI. The
123 main difference is that the EAA forecasts a demand that keeps growing significantly up to
124 2040 while the IAI expects the demand to stagnate more between 2030 and 2040. Even
125 though the methodology behind the projections of the EAA is not elaborately explained in the
126 published report itself, the authors chose to use these numbers because they are the result of

127 more recent research and because they are probably more accurate, since they were
 128 specifically estimated by CRU, a market analysis firm specialised in metals, whereas the
 129 projections of the IAI are based on a relatively simple time series.



130
 131 *Figure 2.1: Additions to the global flow model of the International*
 132 *Aluminium Institute (red: alloy series resolution; green: composition*
 133 *estimate; blue estimate scrap surplus size), based on Bertram et al. (2017)*

134 To overcome these shortcomings, the structural contributions of this paper to the global flow
 135 model of the IAI are threefold. Firstly, it introduces alloy series resolution into the modelled
 136 supply and demand of aluminium. The demand for aluminium ingots, semis, and final
 137 products, as well as the generation of aluminium EOL products, is modelled on an alloy level
 138 in this research, whereas the global flow model of the IAI only estimates the volumes of
 139 aluminium. The flows in red in Figure 2.1 (F11-21) are the ones for which the alloy series
 140 resolution is added. Secondly, whereas the global flow model of the IAI only estimates the
 141 total volumes of generated aluminium scrap, the presented research includes the elemental
 142 composition of the recovered aluminium scrap, based on the estimated amounts of alloys in
 143 recovered EOL products. The flows for which the elemental composition is calculated are
 144 indicated in green (F23-26). The global flow model of the IAI only estimates the volumes of
 145 generated aluminium scrap. Finally, the developed model estimates the size of the generated

146 scrap surplus, which is not considered at all in the global flow model of the IAI. This
147 contribution is indicated in blue (F27). The remainder of the model is unchanged with respect
148 to the original IAI model.

149 The alloy series resolution in the demand for aluminium is introduced by determining each
150 aluminium alloy series' share in the annual aluminium demand per industrial sector. This
151 demand (D_{SECTOR}^{SERIES}) is calculated by multiplying the total demand for aluminium in a sector
152 (D_{SECTOR}), according to the data of the IAI, by the share of that alloy series in the demand of
153 that sector (S_{SECTOR}^{SERIES}), as expressed in Formula 2.1. The annual shares of the alloy series in the
154 total demand for aluminium per sector, considering evolutions in the demand over time, are
155 determined by performing an extensive literature study, as detailed in Appendix 1, combining
156 industry data, governmental data and data published by previous research on aluminium use
157 for all 12 sectors that are defined by the IAI: (1) “Building & Construction”, (2)
158 “Transportation – Auto & Light Truck”, (3) “Transportation – Aerospace”, (4)
159 “Transportation – Other”, (5) “Packaging – Cans”, (6) “Packaging – Other (Foil)”, (7)
160 “Machinery & Equipment”, (8) “Electrical – Cable”, (9) “Electrical – Other”, (10)
161 “Consumer Durables”, (11) “Other (except Destructive Uses)”, and (12) “Destructive Uses”.
162 **Error! Reference source not found.** in Appendix 2 illustrates the shares of the alloy series
163 in the total demand for aluminium in the defined sectors for the year 2020 and indicates on
164 which references the data are based.

$$D_{SECTOR}^{SERIES} = D_{SECTOR} \cdot S_{SECTOR}^{SERIES} \quad (2.1)$$

165 2.2 Scrap Generation

166 Secondary aluminium is sourced from “new scrap” and “old scrap”. New scrap, also referred
167 to as production scrap or pre-consumer scrap, is generated in the manufacturing phase due to
168 process inefficiencies. Old scrap originates from end-of-life products. The annual amounts of

169 new and old scrap collected for recycling from each industrial sector are included in the IAI
 170 data. The developed model requires both the elemental composition of the collected scrap and
 171 the volumes of these scrap flows. In the model's calculations, the composition of the scrap is
 172 first determined on an alloy level and then converted to an elemental level.

173 For new scrap, it is assumed that the generated scrap in a certain year consists of the same
 174 alloys that entered the manufacturing phase that year. As such, the amount of new scrap from
 175 a specific alloy series that is generated in an industrial sector in a specific year

176 ($A_{NEW}^{SERIES,SECTOR}$) can be calculated by multiplying the total amount of generated new scrap in
 177 the sector (A_{NEW}^{SECTOR}) with the share of the alloy series in the demand for aluminium in the
 178 sector (S_{SECTOR}^{SERIES}). The total amount of generated new scrap from a specific alloy series

179 (A_{NEW}^{SERIES}) can be calculated by adding up the amounts of the different sectors. Dividing this
 180 number by the total amount of collected new scrap (A_{NEW}) gives the share of scrap from a
 181 certain alloy series in the total amount of collected new scrap (C_{NEW}^{SERIES}). These calculations

182 are summarised below in Formulas 2.2 to 2.4. Calculating every alloy series' share leads to a
 183 complete alloy level composition of the collected new scrap. This alloy level composition
 184 still has to be converted to an elemental level composition.

$$A_{NEW}^{SERIES,SECTOR} = A_{NEW}^{SECTOR} \cdot S_{SECTOR}^{SERIES} \quad (2.2)$$

$$A_{NEW}^{SERIES} = \sum_{SECTOR} (A_{NEW}^{SECTOR} \cdot S_{SECTOR}^{SERIES}) \quad (2.3)$$

$$C_{NEW}^{SERIES} = A_{NEW}^{SERIES} / A_{NEW} \quad (2.4)$$

185
 186 For old scrap, estimating which alloys can be expected in the collected scrap is more complex
 187 since most aluminium products have a much longer lifetime than one year. Therefore, the
 188 alloys collected from end-of-life products in a specific year are not identical to those that
 189 entered the use phase during that year. The average time aluminium remains “in stock” in the
 190 use phase is estimated by the IAI per sector and region. It varies from one year for packaging

191 to 60 years for aluminium in buildings (Bertram et al., 2017). For the developed MFA model,
192 it is assumed that the alloy series in the scrap of a sector are present in the same proportions
193 as the alloy series that entered the use phase one average lifetime ago for the products in that
194 sector. This assumption does not allow to consider possible variations in the lifetime of the
195 products within a sector. However, this approach still yields reasonable approximations since,
196 in most sectors, the use of alloys in the manufacturing process changes only gradually during
197 the products' average lifetime.

198 With this assumption, the amount of old scrap from a particular alloy series from a certain
199 sector that is collected for recycling ($A_{OLD}^{SERIES,SECTOR}$) can be calculated similarly as for the
200 new scrap (see Formula 2.5). A_{OLD}^{SECTOR} is the amount of old scrap from an industrial sector
201 collected for recycling. Annual numbers for these scrap flows are included in the IAI data, as
202 well as the amount of aluminium end-of-life scrap that is not collected for recycling. This
203 scrap mostly ends up in landfills. The apostrophe in the symbol S'_{SECTOR}^{SERIES} stresses the time
204 delay between the manufacturing phase and the end-of-life phase of the aluminium products
205 in the sector, which must be considered.

206 The total amount of scrap from each alloy series in the collected old scrap from all sectors
207 (A_{OLD}^{SERIES}) can be calculated by summing up the amounts from the different industrial sectors,
208 as expressed in Formula 2.6. An exceptional flow in the developed MFA model is the
209 collected aluminium scrap from used beverage cans (UBC). The researchers that contributed
210 to the global flow model of the IAI indicate that scrap from UBC reaches cast houses mostly
211 separately from casting scrap, extruded scrap, rolled scrap and other scrap from different
212 sources (Bertram et al., 2017). Therefore, UBC recycling is modelled as a closed-loop
213 system, separate from the remainder of the collected scrap. As such, the “Packaging – Cans”
214 sector is not included in the summation of Formula 2.6. The amount of aluminium that has to

215 be produced for this sector with the “conventional” method is reduced by the amount of
 216 closed-loop recycled UBC. Formula 2.7 expresses how the concentration of the scrap from a
 217 particular alloy series in the total amount of collected old scrap (C_{OLD}^{SERIES}) is calculated.
 218 Calculating the concentration of every alloy series leads to a complete alloy level
 219 composition of the collected old scrap. As for the new scrap, this alloy level composition has
 220 to be converted to an elemental level composition.

$$A_{OLD}^{SERIES,SECTOR} = A_{OLD}^{SECTOR} \cdot S_{SECTOR}^{SERIES} \quad (2.5)$$

$$A_{OLD}^{SERIES} = \sum_{SECTOR} (A_{OLD}^{SECTOR} \cdot S_{SECTOR}^{SERIES}) \quad (2.6)$$

$$C_{OLD}^{SERIES} = A_{OLD}^{SERIES} / A_{OLD} \quad (2.7)$$

221

222 2.3 Conversion from alloy level composition to elemental composition

223 To convert the calculated alloy level composition of the new and old scrap to an elemental
 224 composition, it is necessary to know the approximate elemental composition of the different
 225 alloy series. However, the composition of an alloy series is not strictly specified. While all
 226 alloys within a series have the same main alloying element(s), there are still some differences
 227 in composition between specific alloys.

228 In order to come to a generalised elemental composition of each alloy series, the most
 229 popular alloys are selected to represent the average elemental composition of their alloy
 230 series. The selected alloys are listed in the first column of Table 2.1, below the alloy series
 231 they represent. Based on these alloys, the average concentrations of the alloying elements and
 232 impurities are determined for each wrought alloy series and the cast alloys. These
 233 concentrations are given in the “Average” rows of Table 2.1. Combining these concentrations
 234 with the calculated alloy level composition of the collected new and old scrap allows to
 235 calculate the composition of the collected scrap on an elemental level.

236 The concentration of an alloying element in the collected new or old scrap from a certain
 237 sector ($C_{SECTOR,NEW}^{ELEMENT}$) can be calculated with Formulas 2.8 and 2.9. The symbol $C_{SERIES}^{ELEMENT}$
 238 stands for the values in the “Average” rows of Table 2.1. The mass of an alloying element in
 239 the total amount of collected scrap can be calculated with Formula 2.10. Dividing this value
 240 by the total mass of all collected scrap, except for the collected UBC, gives the concentration
 241 of the alloying element in the total amount of collected scrap (see Formula 2.11). Calculating
 242 the concentrations of all alloying elements and impurities gives a complete composition of
 243 the collected scrap on an elemental level.

$$C_{SECTOR,NEW}^{ELEMENT} = \sum_{SERIES} (0.01 \cdot C_{SERIES}^{ELEMENT} \cdot S_{SECTOR}^{SERIES}) \quad (2.8)$$

$$C_{SECTOR,OLD}^{ELEMENT} = \sum_{SERIES} (0.01 \cdot C_{SERIES}^{ELEMENT} \cdot S'_{SECTOR}^{SERIES}) \quad (2.9)$$

$$A_{ALL\ SCRAP}^{ELEMENT} = \sum_{SERIES} ((A_{NEW}^{SERIES} + A_{OLD}^{SERIES}) \cdot 0.01 \cdot C_{SERIES}^{ELEMENT}) \quad (2.10)$$

$$C_{ALL\ SCRAP}^{ELEMENT} = A_{ALL\ SCRAP}^{ELEMENT} / (A_{NEW} + A_{OLD}) \quad (2.11)$$

244 2.4 Supply of Aluminium

245 Aluminium products are manufactured from a mixture of primary and secondary aluminium.
 246 Due to the presence of alloying elements and impurities in the collected scrap, the capacity of
 247 wrought alloys to absorb secondary aluminium is limited. The recycled content of the
 248 wrought alloy series (this is the allowable mass fraction of secondary aluminium in the
 249 mixture of primary and secondary aluminium used to produce wrought alloys) can be
 250 calculated based on the calculated composition of the collected scrap and the estimated
 251 tolerances for impurities of the wrought alloy series. Aluminium alloys have an allowable
 252 range of concentrations for alloying elements and impurities. The tolerance of an aluminium
 253 alloy for an element is defined here as the maximum allowable concentration of that element
 254 in the aluminium alloy. As for the average concentration, the tolerances of an alloy series are

255 not strictly specified. Therefore, the tolerance of an alloy series for an element is determined
256 in this research by selecting the lowest tolerance for that element among the representative
257 alloys listed in Table 2.1. The resulting tolerances (“Tol”) of the wrought alloy series for the
258 different alloying elements and impurities can be found in the last row of each alloy series in
259 Table 2.1.

Table 2.1: Concentrations and Tolerances for Alloying Elements and Impurities of the Wrought Alloy Series and Cast Alloys based on (Aircraft Materials, 2020; AZO Materials 2005, 2013; MakeItFrom, 2020; Matweb, 2020)

Alloy series (representative alloys)	Statistic	Cu (wt%)	Fe (wt%)	Mg (wt%)	Mn (wt%)	Si (wt%)	Zn (wt%)	Other (wt%)
1000 (1050, 1100, 1200)	Min	0	0	0	0	0	0	0
	Max	0.20	1.00	0.05	0.05	1.00	0.10	0.15
	Average	0.05	0.20	0.04	0.02	0.20	0.05	0.10
	Tol	0.05	0.40	0.05	0.05	0.25	0.05	0.06
2000 (2014, 2024, 2025)	Min	3.80	0	0	0.30	0	0	0
	Max	5.00	1.00	1.80	1.20	1.20	0.25	0.15
	Average	4.50	0.20	1.00	0.50	0.60	0.10	0.10
	Tol	4.90	0.50	0.05	0.90	0.50	0.25	0.15
3000 (3004)	Min	0	0	0.80	1.00	0	0	0
	Max	0.25	0.70	1.30	1.50	0.30	0.25	0.15
	Average	0.10	0.50	1.10	1.30	0.15	0.10	0.10
	Tol	0.25	0.70	1.30	1.50	0.30	0.25	0.15
4000 (4043)	Min	0	0	0	0	4.50	0	0
	Max	0.30	0.80	0.05	0.05	6.00	0.10	0.15
	Average	0.10	0.20	0.03	0.03	5.20	0.05	0.10
	Tol	0.30	0.80	0.05	0.05	6.00	0.10	0.15
5000 (5005, 5052, 5083)	Min	0	0	0.50	0	0	0	0
	Max	0.20	0.70	5.00	0.20	0.40	0.25	0.15
	Average	0.05	0.20	3.00	0.10	0.25	0.10	0.10
	Tol	0.10	0.35	1.10	0.10	0.25	0.10	0.15
6000 (6061, 6063, 6082)	Min	0	0	0.45	0	0.20	0	0
	Max	0.40	0.70	1.20	1.00	1.30	0.25	0.15
	Average	0.20	0.30	1.10	0.30	0.70	0.10	0.10
	Tol	0.10	0.35	0.90	0.10	0.60	0.10	0.15
7000 (7050, 7075, 7475)	Min	1.20	0	1.90	0	0	5.10	0
	Max	2.60	0.50	2.90	0.30	0.40	6.70	0.25
	Average	1.80	0.30	2.40	0.10	0.10	6.00	0.20
	Tol	1.90	0.12	2.60	0.06	0.10	6.10	0.15
8000 (8176)	Min	0	0.40	0	0	0.03	0	0
	Max	0.05	1.00	0.05	0.05	0.15	0.10	0.15
	Average	0.05	0.70	0.05	0.05	0.10	0.05	0.10
	Tol	0.05	1.00	0.05	0.05	0.15	0.10	0.15
Cast alloys (319, 356, 380)	Average	2.50	0.60	0.30	0.30	7.10	1.20	0.30

260

261 A conservative specification of the tolerances is deliberately introduced to ensure that the

262 allowable recycled content of the wrought alloy series is not overestimated. It should be

263 considered that old scrap is always contaminated to some extent with other materials,
264 resulting from separation errors, imperfect liberation of laminated or shape included materials
265 and unliberated joints. Previous research has demonstrated that aluminium output fractions in
266 state-of-the-art recycling facilities consist for 98.11 wt% to 99.57 wt% of aluminium alloys,
267 depending on the size to which the material is shredded (Soo et al., 2018). Similar results are
268 achieved by manual sorting by well trained workers (Capuzzi and Timelli, 2018). According
269 to Soo et al. (2018), the majority (0.23-0.96 wt%) of the contaminatons in aluminium scrap is
270 of an organic nature and, depending on the size of the shredded material, 0.03 wt% up to
271 0.36% is iron and 0.13 wt% up to 0.26 wt% is copper. These contaminants come on top of the
272 amount of iron and copper that is present in the form of alloying elements in the aluminium
273 scrap. Increasing the estimated amount of iron and copper in the recovered scrap to take into
274 account these contaminants would require extrapolating the data that were acquired by Soo et
275 al. (2018). Since this approach would result in increased complexity of the model and
276 introduce additional uncertainty, the authors instead opted to use a more conservative
277 specification of the tolerances to ensure that the allowable recycled content of the wrought
278 alloy series is not overestimated.

279 The limit that the presence of an alloying element imposes on the use of secondary
280 aluminium to produce a wrought alloy series ($L_{SERIES}^{ELEMENT}$) is calculated by dividing the alloy
281 series' tolerance for the element by the concentration of the element in the collected scrap
282 (see Formula 2.12). The collected scrap is assumed to be a mix of both old and new scrap
283 from all sectors. Each alloying element imposes a limit ($L_{SERIES}^{ELEMENT}$) on the use of secondary
284 aluminium for the production of the wrought alloy series. The maximum recycled content of
285 a wrought alloy series ($RC^{WR.SER}$) equals the lowest of the limits imposed by the different
286 alloying elements in the scrap. This value indicates the mass percentage of secondary
287 aluminium that can be used in the production of each wrought alloy series, and the

288 complement of this value is the mass percentage of primary aluminium necessary for diluting
289 the scrap.

$$L_{SERIES}^{ELEMENT} = 0.01 \cdot T_{SERIES}^{ELEMENT} / C_{ALL\ SCRAP}^{ELEMENT} \quad (2.12)$$

290

291 Cast alloys have a very high capacity to absorb recycled material. Recycled aluminium can
292 constitute 99.3 wt% or even more of the total aluminium mass in typical applications for cast
293 alloys (Paraskevas et al., 2015). Modaresi et al. (2014) neglect the required aluminium for
294 diluting cast alloys in their calculations to predict the emergence of a scrap surplus since this
295 simplification only has a minimal impact on the overall result. For the same reason, this tiny
296 fraction of primary aluminium that has to be added to recycled aluminium for the production
297 of cast alloys is neglected in the developed model, and the maximum recycled content of cast
298 alloys is, therefore, considered to be 100%.

299 The amount of secondary aluminium that can be used to produce new alloys is slightly lower
300 than the amount of collected scrap due to premelting and melting losses during recycling. The
301 IAI holds data on these losses involved in the recycling process of old and new scrap.

302 According to the IAI, old scrap premelting recovery rates are consistently higher than 97%
303 for any sector in any year, while old scrap melting recovery rates go as low as 85% for
304 aluminium foil in the earlier years of the investigated time frame. For new scrap, premelting
305 losses are neglected, and the melting recovery rate is estimated at 98% for each sector and
306 each year. Considering these rates, the amounts of primary and secondary aluminium used in
307 the production of the different alloy series and the scrap surplus size can be calculated.

308 The amount of secondary aluminium that can be used for the production of each wrought
309 alloy series ($S_{SEC}^{WR.SER}$) is calculated by multiplying the global demand for the alloy series
310 ($D^{WR.SER}$), as determined in Section 2.1, by its recycled content ($RC^{WR.SER}$). The amount of
311 primary aluminium that flows to each wrought alloy series ($S_{PRI}^{WR.SER}$) is the difference

312 between the demand for the wrought alloy series ($D^{WR.SER}$) and the amount of recycled
313 aluminium that flows to the alloy series ($S_{SEC}^{WR.SER}$). As long as the amount of generated
314 aluminium scrap that is not used for wrought alloy production is smaller than the demand for
315 cast alloys, there is no scrap surplus (SP). In this case, the scrap that is not used for wrought
316 alloy production can be absorbed entirely by the cast alloys. The amount of primary
317 aluminium used in the production of the cast alloys (S_{PRI}^{CAST}) is then equal to the difference
318 between the demand for cast alloys (D^{CAST}) and the amount of secondary aluminium used in
319 the production of cast alloys (S_{SEC}^{CAST}). However, if the amount of recycled aluminium exceeds
320 the capacity of both wrought and cast alloys to absorb this material, there is no destination
321 left for this flow. Then, the size of the scrap surplus is equal to the generated amount of scrap
322 after melting and premelting losses (A'_{SEC}) minus the demand for cast alloys and the amount
323 of secondary aluminium used in wrought alloy production. These calculations are
324 summarised in Formulas 2.13 to 2.17. All the model calculations have been made in a
325 Microsoft Excel Workbook and are visualised in the form of a Sankey diagram using the
326 Python programming language and the FloWeaver library (Lupton and Allwood, 2017;
327 Lupton, 2017).

$$S_{SEC}^{WR.SER} = RC^{WR.SER} \cdot D^{WR.SER} \quad (2.13)$$

$$S_{PRI}^{WR.SER} = D^{WR.SER} - S_{SEC}^{WR.SER} \quad (2.14)$$

$$S_{SEC}^{CAST} = \begin{cases} A'_{SEC} - \sum_{SERIES} S_{SEC}^{WR.SER} & \text{if } A'_{SEC} - \sum_{SERIES} S_{SEC}^{WR.SER} < D^{CAST} \\ D^{CAST} & \text{if } A'_{SEC} - \sum_{SERIES} S_{SEC}^{WR.SER} > D^{CAST} \end{cases} \quad (2.15)$$

$$S_{PRI}^{CAST} = \begin{cases} D^{CAST} - \left(A'_{SEC} - \sum_{SERIES} S_{SEC}^{WR.SER} \right) & \text{if } A'_{SEC} - \sum_{SERIES} S_{SEC}^{WR.SER} < D^{CAST} \\ 0 & \text{if } A'_{SEC} - \sum_{SERIES} S_{SEC}^{WR.SER} > D^{CAST} \end{cases} \quad (2.16)$$

$$SP = \begin{cases} 0 & \text{if } A'_{SEC} - \sum_{SERIES} S_{SEC}^{WR.SER} < D^{CAST} \\ A'_{SEC} - D^{CAST} - \sum_{SERIES} S_{SEC}^{WR.SER} & \text{if } A'_{SEC} - \sum_{SERIES} S_{SEC}^{WR.SER} > D^{CAST} \end{cases} \quad (2.17)$$

328

329 2.5 Aluminium Scrap Sampling

330 The demand for aluminium alloys and the composition of the collected aluminium scrap are
331 calculated in the model based on data from literature. To be able to compare the literature
332 data with the actual composition of aluminium scrap collected at recycling facilities,
333 composition measurements have been conducted on aluminium scrap samples collected at a
334 Belgian recycling facility. A batch of 275 aluminium scrap samples with a total mass of over
335 10 kg was collected from the so called “Twitch (40-120 mm)” fraction at the recycling
336 facility of Galloo in Menen, Belgium. This fraction consists almost exclusively of aluminium
337 scrap. The aluminium in the Twitch fraction of Galloo is separated from other materials in the
338 treated end-of-life waste streams by magnetic separation, density separation, eddy current
339 separation, and optical separation (Eggers et al., 2019). According to the representatives of
340 Galloo, the aluminium in the Twitch fraction originates on average for 40% from
341 construction waste, for 40% from automotive waste and for 20% from waste from consumer
342 durables.

343 The composition of the collected samples was measured with a handheld XRF device
344 (Thermo Scientific Niton XL2). Based on the XRF measurements, the 275 samples were
345 divided in five categories related to their alloy type. The 1000 series, 3000 series, and cast
346 alloys are three separate categories. The 2000, 4000, 7000, and 8000 series alloys are
347 combined in the “Other Wrought” category since they are significantly less popular than the
348 other series and barely encountered during the measurements. The alloys of the 5000 and
349 6000 series are bundled in one category due to the difficulty of distinguishing between these
350 series with the used measuring method.

351 2.6 Method for sensitivity analysis

352 Predicting the composition of the global aluminium flows and the size of the scrap surplus
353 involves considerable uncertainties. Since the evolution of the scrap surplus is estimated by
354 expanding the IAI's global flow model, not only the uncertainties that arise from the
355 assumptions in this paper have to be considered, but also the uncertain parameters within the
356 IAI model. Two sources of uncertainty that are introduced in this paper and that have a
357 particularly high influence on the scrap surplus growth are the changing demand for cast
358 alloys in the automotive sector and the composition of the collected scrap. The estimated
359 demand for cast alloys in the automotive sector in the presented MFA model relies on the
360 projections of Modaresi et al. (2014). However, predictions for the future demand of cast
361 alloys for cars and light trucks vary significantly, depending on the consulted source, due to
362 the considerable uncertainty in the rate at which electric vehicles will gain market share in the
363 automotive sector in the coming decades (Hatayama et al., 2012; Buchner et al., 2017).
364 Furthermore, the most critical parameter within the global flow model of the IAI is the
365 lifetime of the products in the different sectors. To show how the estimated evolution of the
366 scrap surplus is affected by these different uncertainties in the data, a scenario-based
367 sensitivity analysis is performed.

368 Seven alternative scenarios are investigated in addition to the baseline scenario. In the first
369 alternative scenario ("slow electrification"), the share of cast alloys in the aluminium demand
370 in the automotive sector diverges gradually from the share assumed in the baseline scenario
371 between 2020 and 2040. In 2020, this share is still assumed the same as in the baseline
372 scenario, but it linearly increases until 2040 when it is ten percentage points higher than in
373 the baseline scenario. This increased demand for cast alloys corresponds to a situation in
374 which the transition towards electric vehicles takes place slower than anticipated in the
375 baseline scenario. In the second alternative scenario ("fast electrification"), the share of cast

376 alloys in the automotive sector's aluminium demand is gradually decreased from 2020
377 onwards until it is ten percentage points lower than in the baseline scenario in 2040. This
378 scenario represents a faster than anticipated electrification in the automotive sector.

379 The third and fourth alternative scenarios illustrate the influence of the composition of the
380 collected aluminium scrap. In the baseline scenario, the secondary scrap composition is
381 calculated based on the average concentration of alloying elements in the wrought alloys, as
382 presented in the "Average" rows of Table 2.1. In the third ("Min Alloys") and fourth ("Max
383 Alloys") alternative scenarios, the secondary scrap composition is calculated based on the
384 values in the "Min" and "Max" rows in Table 2.2, respectively. In the third alternative
385 scenario, an alloying element's concentration in an alloy is assumed to be 0.01wt% when no
386 lower limit is specified for the production of that alloy. This is a very low value, even for
387 wrought alloys, and considered the minimum concentration of an alloying element in
388 collected scrap since, in a realistic instance, the average concentration of alloying elements
389 and impurities will never be exactly zero. This specification is important to avoid too
390 unrealistic values in this scenario. These two scenarios also offer an idea about the magnitude
391 of the change in the size of the scrap surplus that results from the presence of tramp elements
392 in the collected aluminium scrap. According to Soo et al. (2018), the iron and copper
393 impurities due to tramp elements account for 0.03wt% to 0.36wt% and 0.13wt% to 0.26wt%
394 of the aluminium scrap, respectively. In the third and fourth alternative scenario, the
395 considered deviations in the iron and copper content are slightly larger than these numbers.
396 Therefore, the considered deviations in these scenarios cover the range of impurity
397 concentrations that can be realistically expected in aluminium scrap.

398 The fifth alternative scenario ("Galoo") considers the results of the scrap measurements.
399 Whereas in the baseline scenario, the alloy-level composition of the scrap from the sectors
400 "Building & Construction", "Transportation – Auto & Light Truck", and "Consumer

401 Durables” is determined based on literature data, in this alternative scenario the compositions
 402 are adjusted so that they match the results of the scrap measurements. The estimated share of
 403 the 1000 series, 3000 series, and cast alloys in the recovered scrap is increased, while the
 404 share of 5000, 6000, and 7000 series alloys is decreased with respect to the literature data.
 405 The purpose of including this scenario is to demonstrate the sensitivity of the scrap surplus
 406 growth to the alloy-level composition of the collected old scrap.

407 To demonstrate the sensitivity of the scrap surplus evolution to the product lifetimes assumed
 408 in the IAI global flow model, a sixth and seventh alternative scenario have been developed.
 409 In the global flow model, global average lifetimes of aluminium products are estimated per
 410 sector (see Appendix 3). In the sixth scenario, these average lifetimes are reduced in a linear
 411 way with 10% between 2020 and 2040. In the seventh alternative scenario, the average
 412 lifetimes are reduced in a linear way by 20% between 2020 and 2040.

413 3 Results & Discussion

414 3.1 Limits to recycled content for wrought alloys

415 Table 3.1 shows the limit that each element in the collected aluminium scrap imposes on the
 416 recycled content of the different wrought alloy series ($L_{SERIES}^{ELEMENT}$) in 2020. The recycled
 417 content ($RC^{WR.SER}$), the most critical limit for each alloy series, is marked in yellow.

418 *Table 3.1 Calculated Upper Limits for the Recycled Content of the Wrought*
 419 *Alloy Series in 2020*

Element	1000	2000	3000	4000	5000	6000	7000	8000
Cu	5%	100%	26%	31%	10%	10%	100%	5%
Fe	100%	100%	100%	100%	93%	93%	32%	100%
Mg	4%	4%	100%	4%	100%	89%	100%	4%
Mn	17%	100%	100%	17%	34%	34%	20%	17%
Si	9%	19%	11%	100%	10%	23%	4%	5%
Zn	8%	42%	42%	16%	16%	16%	10%	16%
Other	36%	90%	90%	90%	90%	90%	90%	90%

420

421 3.2 Sankey diagram

422 Figure 3.1 shows the Sankey diagram for the calculated aluminium flows in 2030. Diagrams
423 for 2035 and 2040 are included in Appendix 4. In the Sankey diagram, the nodes are ordered
424 according to the different lifecycle stages, and the colors indicate the alloy series or the type
425 of aluminium that flows between the nodes. The scrap from UBC is recycled in a closed-loop
426 recycling scheme, in contrast to the aluminium flows for the other end-of-life products. The
427 scrap surplus is represented as a flow that starts in the supply phase, which cannot be
428 connected to the manufacturing phase.

429 According to the model's calculations, the scrap surplus would constitute 11.4% of all
430 collected aluminium scrap in 2030. This would mean that in 2030, only 88.6% of all collected
431 and processed aluminium scrap could be used for the production of new wrought and cast
432 alloys. By 2040, this share is estimated to decline to 84.0%. In such situation, the use of
433 primary aluminium would continue to grow despite the abundant availability of aluminium
434 scrap.

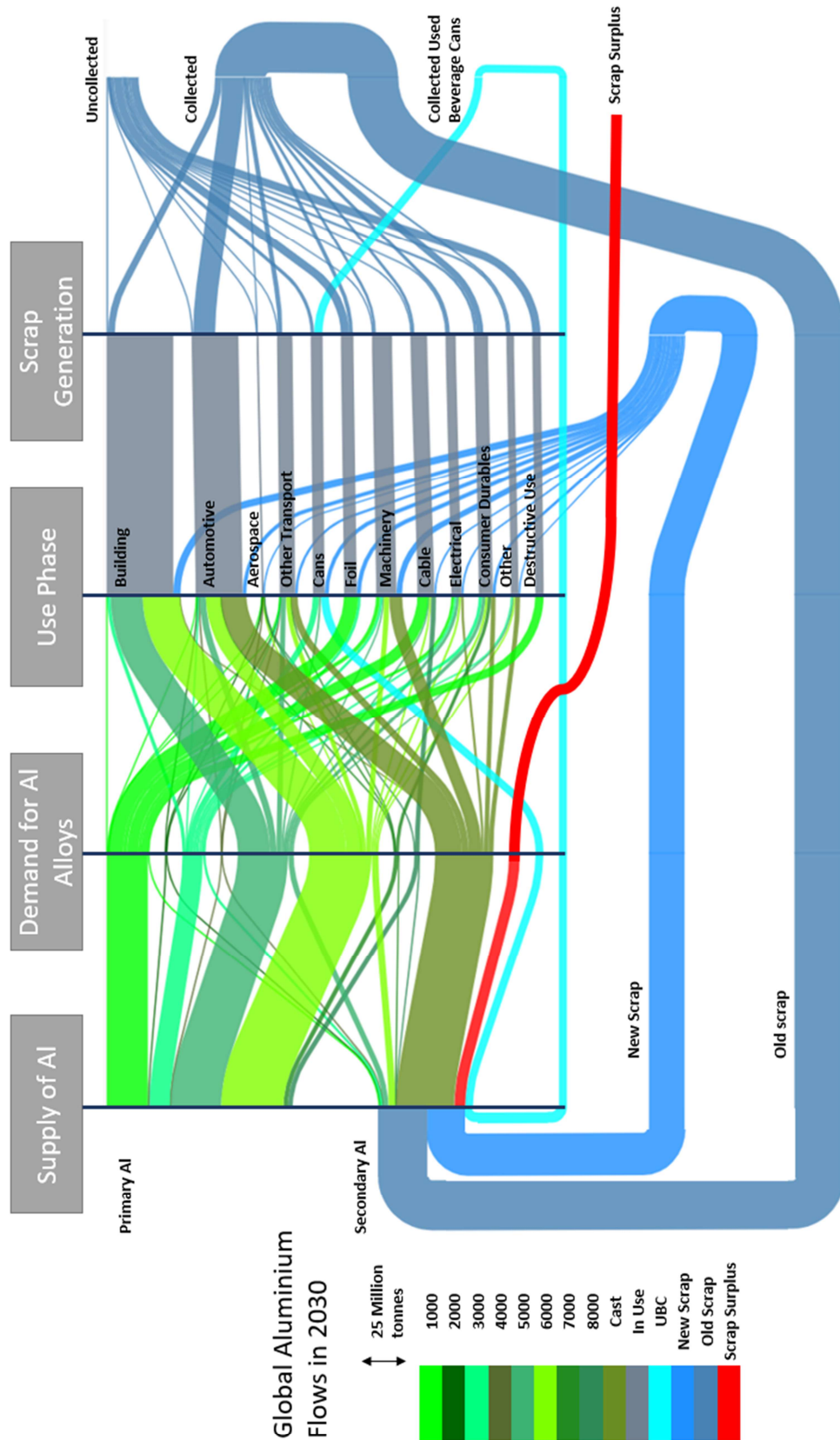


Figure 3.1: Sankey diagram representing the global aluminium flows in 2030, shades of green represent the alloy series (1000-8000 + cast), data in Appendix 5

435 3.3 Composition Measurements

436 Figure 3.2 shows the measured shares of the different alloy series in the set of aluminium
437 (Twitch) scrap samples collected at Galloo, as well as the model's prediction for the
438 composition of old scrap collected in 2020 from a mix of 40% scrap from construction, 40%
439 automotive scrap and 20% scrap from consumer durables. The measured share of cast alloys
440 in the Twitch fraction is relatively close to the estimated share. Among the wrought alloys,
441 there are significant differences between the measured and estimated shares of the different
442 alloy series. There are multiple explanations for these differences. First of all, it could be that
443 the gathered sample does not exactly reflect the average composition of the Twitch fraction
444 over the course of one year. The assumed origins of the measured scrap (40% construction,
445 40% automotive, and 20% consumer durables) are a company estimate of yearly averages.
446 However, the composition of the scrap varies significantly throughout the year. Another
447 important consideration is that the global average composition of a mix of old scrap is
448 compared with the composition of the scrap at a local Belgian recycling facility. Since there
449 are regional differences in the use of alloys for the production of aluminium products, it is not
450 unexpected that the scrap collected in Belgium has a slightly different composition than the
451 global average. The importance of an accurate estimate of the collected scrap's alloy-level
452 composition for estimating the growth of the scrap surplus is shown in the sensitivity analysis
453 in the next section.

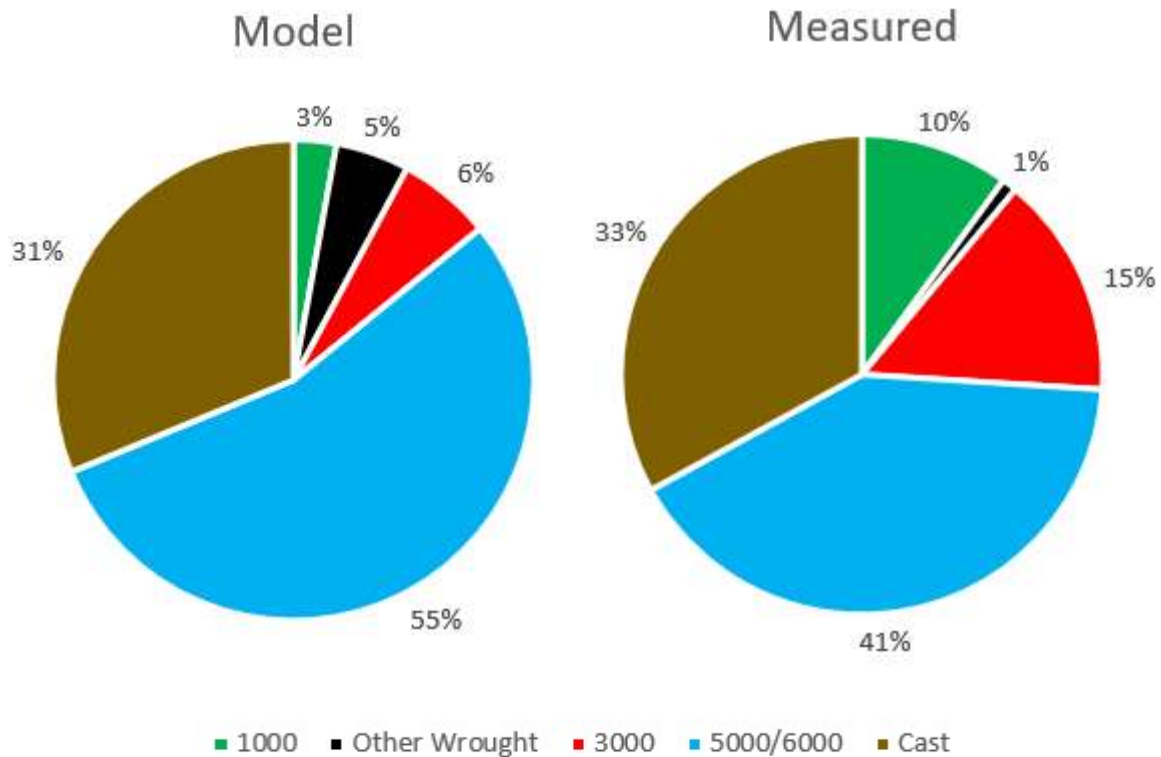


Figure 3.2: Alloy-level composition of collected scrap: Predicted by Model and Measured

454 3.4 Scenario-based sensitivity analysis for the evolution of the scrap surplus

455 **Error! Reference source not found.** shows the estimated evolution of the global scrap

456 surplus between 2020 and 2040. In this figure, the baseline scenario of the predicted

457 evolution is compared to seven other scenarios. These scenarios demonstrate the sensitivity

458 of the scrap surplus's growth to the most important sources of uncertainty in the model.

459 According to the calculations in the baseline scenario, a small global scrap surplus of 0.5

460 million tonnes first surfaced for one year in 2009, the year that the global economy contracted

461 by almost 2% (The World Bank, 2021). In this year of recession, the London Metal Exchange

462 suffered significant financial losses when its stock of aluminium increased by 152% in one

463 year to 2.34 million tonnes (Salazar and McNutt, 2010). However, it is difficult to prove the

464 scrap surplus's contribution to this incident since the most significant part of these stocks was

465 probably the result of the overproduction of primary aluminium, as the sudden collapse in

466 demand took many aluminium producers by surprise. Starting from 2023, an annual global

467 scrap surplus is predicted to arise and to continue to grow quickly to 5.4 million tonnes of
 468 aluminium in 2030 and then to around 8.7 million tonnes in 2040. This prediction is
 469 relatively close to what other researchers have predicted (Hatayama et al., 2008, 2012;
 470 Modaresi and Müller, 2012; Modaresi et al., 2014). There is a kink in the scrap surplus
 471 evolution in the year 2030, due to the decrease in the annual growth rate of the demand for
 472 aluminium that is expected by the EAA. As a consequence, the generated amount of new
 473 scrap and the amount of old scrap from products with very short lifetimes increase less
 474 rapidly.

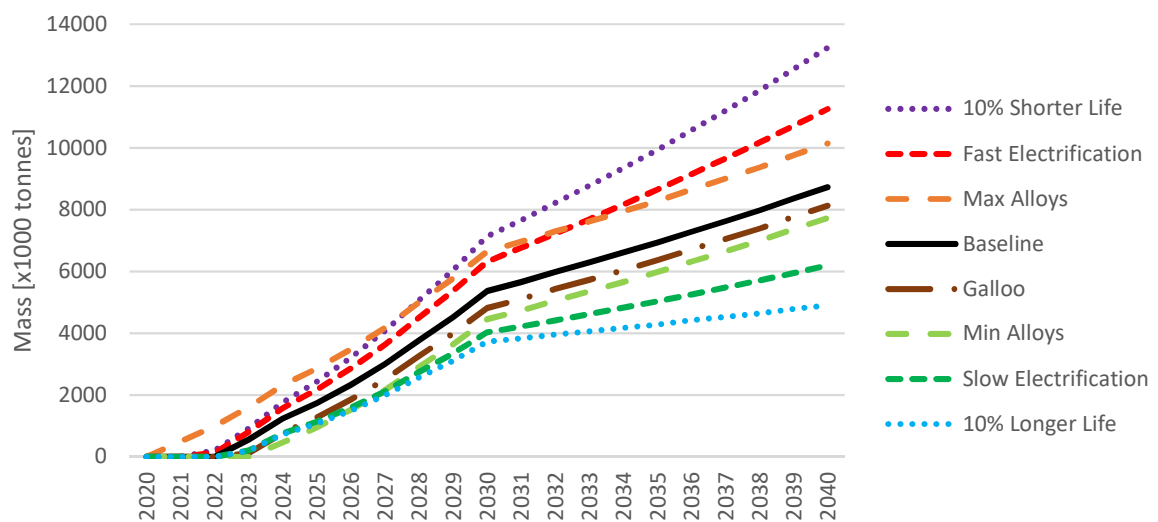


Figure 3.3: Sensitivity analysis for the evolution of the annual global aluminium scrap surplus, data in Appendix 5

475 Figure 3.3 shows that both the demand for cast alloys in the automotive sector and the
 476 amount of alloying elements in the collected scrap have a significant influence on the scrap
 477 surplus growth. The “Galloo” scenario lies relatively close to the baseline scenario, even
 478 though there are significant differences between the measured alloy-level composition of the
 479 collected scrap at Galloo and the alloy-level composition predicted from literature data.
 480 Figure 3.2 showed that, especially among the wrought alloys, the predicted and measured

481 composition differed somewhat, while the shares of the cast alloys were very similar. The
482 fact that the “Galoo” scenario lies closer to the baseline scenario than the other alternative
483 scenarios indicates therefore that, for predicting the evolution of the scrap surplus, it is most
484 important to accurately determine the demand for cast alloys and the amount of cast alloys in
485 the collected scrap. Relatively small deviations in the shares of the wrought alloy series in the
486 composition of the scrap affect the scrap surplus much less. This is because the compositional
487 differences between the most popular wrought alloy series are much smaller than the
488 compositional difference between wrought and cast alloys in general.

489 The lifetime of the aluminium products also has a major influence on the evolution of the
490 scrap surplus. A linear decrease of 10% between 2020 and 2040 in the aluminium product
491 lifetimes adds 4.5 million tonnes to the global scrap surplus by 2040 with respect to the
492 baseline scenario. A linear increase of 10% in the product lifetimes between 2020 and 2040
493 leads to a 3.8 million tonnes decrease in the size of the annual global scrap surplus by 2040.
494 These results show that if the lifetime of aluminium products would decrease more rapidly
495 than expected, the scrap surplus would grow even faster. Such trend is not unthinkable, since
496 according to the IAI the average lifetime of aluminium products in the automotive sector is
497 already significantly below average (20 years) in regions such as Europe and North-America
498 (15 years), and Japan and the Middle-East (12 years). In China, the estimated lifetime of
499 aluminium products in the building sector is as short as 30 years, compared to a global
500 average of 50 years (Bertram et al., 2017). Furthermore, it should be considered that future
501 initiatives promoting the renovation of buildings and the replacement of older vehicles with
502 higher emissions for the sake of the environment could even further decrease the average
503 functional lifetime of aluminium products. Finally, it is also important to consider that the
504 mentioned sources of uncertainty can be combined. For example, a faster electrification of
505 the automotive sector could occur simultaneously as a decrease in the functional lifetime of

506 aluminium products. In that case, the scrap surplus would be even higher than in the
507 documented scenarios.

508 The economic consequences of the Covid-19 (C19) pandemic have added another source of
509 uncertainty to the estimate of the scrap surplus evolution. The demand forecasts used as input
510 for the developed model are based on pre-C19 studies. 85% of the stakeholders interviewed
511 by the IAI believe that the demand for aluminium will rebound to these pre-C19 levels by the
512 end of 2021 (CM Group, 2020). Therefore, the authors expect that the C19 pandemic will
513 have only a limited effect on the presented estimate beyond 2022. In any case, only the input
514 data of the developed model have to be updated to compute a new estimate based on
515 information gathered after the outbreak of C19.

516 Since the results of the model developed in this paper, as well as the results from other
517 researchers, indicate that the emergence of a scrap surplus is imminent, the authors
518 recommend that the IAI adopts a more thorough methodology for its global aluminium flow
519 model. While it is already highly informative in its current form, it lacks the level of detail
520 needed to estimate the scrap surplus evolution and the demand for specific alloys. The
521 methodology, data, and results presented in this paper provide a possible starting point for the
522 IAI to refine its global flow model.

523 4 Conclusions and future work

524 The presented research demonstrates that an aluminium scrap surplus will emerge in the
525 coming decade if the aluminium recycling industry does not adopt enhanced sorting systems
526 or improved recycling strategies. The developed MFA model estimates that a scrap surplus
527 will emerge in the coming years and that its size will grow to 5.4 million tonnes in 2030 and
528 to 8.7 million tonnes in 2040. Without countermeasures, the inability to recycle this amount
529 of aluminium scrap will necessitate an additional increase in primary aluminium production,

530 which has a highly negative economic and environmental impact. The scenario-based
531 sensitivity analysis shows that the evolution of the scrap surplus strongly depends on both the
532 demand for cast alloys and the composition of the collected scrap. Composition
533 measurements have been conducted on old scrap collected by a large Belgian recycling
534 facility. The results are used in the sensitivity analysis to demonstrate how the estimated
535 evolution of the scrap surplus is impacted by small deviations in the shares of the wrought
536 alloy series in the collected aluminium scrap.

537 The level of detail of the IAI's global aluminium flow model could be increased by adopting
538 the presented methodology. The relevance of tracking and estimating the global aluminium
539 flows at alloy series level will only increase in the near future, as the aluminium industry will
540 adapt the current methods of sorting and recycling aluminium scrap to increase the recycled
541 content of wrought aluminium products. In future work, several methods to enhance current
542 sorting and recycling practices will be investigated. Promising strategies to increase the
543 recycled content of aluminium products are closed-loop recycling of aluminium products,
544 separating old scrap from new scrap, and enhanced alloy-based sorting. The authors will
545 investigate the benefits of separately processing waste streams of different sectors and the use
546 of LIBS (Laser Induced Breakdown Spectroscopy) in combination with computer vision to
547 sort old aluminium scrap at alloy series level. The extent to which these technologies can
548 mitigate the growth of the global aluminium scrap surplus remains an important question,
549 which the authors will also assess in future work, starting from the results of this paper.

550 5 Acknowledgements

551 This work has received funding from the European Institute of Innovation and Technology
552 (EIT), a body of the European Union, under the Horizon 2020, the EU Framework

- 553 Programme for Research and Innovation in the AUtomatic SOrting of mixed scrap Metals
- 554 (AUSOM) project (project number 19294, <https://www.ausomproject.eu/>).

555 Bibliography

- 556 Aircraft Materials, 2020. Alloy 4043/ Aluminium Welding Alloy 4043.
557 <https://www.aircraftmaterials.com/data/weld/4043.html> (accessed: Apr. 09, 2021).
- 558 Allwood, J.M., Cullen, J.M., 2012. Sustainable Materials - with both eyes open : Future
559 Buildings, Vehicles, Products and Equipment - Made Efficiently and Made with Less
560 New Material, 1st ed. Cambridge, United Kingdom.
561 [https://www.bookdepository.com/Sustainable-Materials-with-both-eyes-open-Julian-](https://www.bookdepository.com/Sustainable-Materials-with-both-eyes-open-Julian-Allwood/9781906860073)
562 [Allwood/9781906860073](https://www.bookdepository.com/Sustainable-Materials-with-both-eyes-open-Julian-Allwood/9781906860073) (accessed: Apr. 09, 2021)
- 563 Auxier, G.W., 1953. Aluminum and magnesium : history of the Aluminum and Magnesium
564 Division of the National Production Authority. Washington, DC, USA: U.S. Dept. of
565 Commerce, National Production Authority.
566 <https://catalog.hathitrust.org/Record/102381795> (accessed: Apr. 09, 2021)
- 567 Avallone, E.A., Baumeister, T., Sadegh, A.M., 2006. Marks' standard handbook for
568 mechanical engineers, 11th ed. McGraw-Hill Professional Pub.
569 [https://www.abebooks.com/9780071428675/Marks-Standard-Handbook-Mechanical-](https://www.abebooks.com/9780071428675/Marks-Standard-Handbook-Mechanical-Engineers-0071428674/plp)
570 [Engineers-0071428674/plp](https://www.abebooks.com/9780071428675/Marks-Standard-Handbook-Mechanical-Engineers-0071428674/plp) (accessed: Apr. 09, 2021)
- 571 AZO Materials, 2005. Aluminium Alloys - Aluminium 5083 Properties, Fabrication and
572 Applications. <https://www.azom.com/article.aspx?ArticleID=2804> (accessed: Apr. 09,
573 2021)
- 574 AZO Materials, 2013. Aluminum 8176 Alloy (UNS A98176).
575 <https://www.azom.com/article.aspx?ArticleID=8788> (accessed: Apr. 09, 2021).
- 576 Belan, J., Vaško, A., Kuchariková, L., 2018. A brief overview and metallography for
577 commonly used materials in aero jet engine construction. Production Engineering
578 Archives, vol. 17, pp. 8–13. <https://doi.org/10.30657/pea.2017.17.02>

579 Bertram, M., Martchek, K.J., Rombach, G., 2009. Material Flow Analysis in the Aluminum
580 Industry. *Journal of industrial ecology*, vol. 13, no. 5, pp. 650–654.
581 <https://doi.org/10.1111/j.1530-9290.2009.00158.x>.

582 Bertram, M., Ramkumar, S., Rechberger, H., Rombach, G., Bayliss, C., Martchek, K.J.,
583 Müller, D.B., Liu, G., 2017. A regionally-linked, dynamic material flow modelling tool
584 for rolled, extruded and cast aluminium products. *Resources, conservation and recycling*,
585 vol. 125, pp. 48–69. <https://doi.org/10.1016/j.resconrec.2017.05.014>.

586 BloombergNEF, 2019. Electric Vehicle Outlook 2019. [https://about.bnef.com/electric-](https://about.bnef.com/electric-vehicle-outlook/#toc-viewreport)
587 [vehicle-outlook/#toc-viewreport](https://about.bnef.com/electric-vehicle-outlook/#toc-viewreport) (accessed: Apr. 07, 2020)

588 Buchner, H., Laner, D., Rechberger, H., Fellner, J., 2017. Potential recycling constraints due
589 to future supply and demand of wrought and cast Al scrap - A closed system perspective
590 on Austria. *Resources, conservation and recycling*, vol. 122, pp. 135–142.
591 <https://doi.org/10.1016/j.resconrec.2017.01.014>.

592 Campbell, F.C., 2006. *Manufacturing Technology for Aerospace Structural Materials*, 1st ed.
593 Oxford, United Kingdom, 2006. <https://doi.org/10.1016/B978-1-85617-495-4.X5000-8>.

594 Capuzzi, S., Timelli, G., 2018. Preparation and Melting of Scrap in Aluminum Recycling: A
595 Review. *Metals - Open Access Metallurgy Journal*, vol. 8.
596 <http://dx.doi.org/10.3390/met8040249>

597 Chen, G., Wang, X., Wang, J., Liu, J., Zhang, T., Tang, W., 2012. Damage investigation of
598 the aged aluminium cable steel reinforced (ACSR) conductors in a high-voltage
599 transmission line. *Engineering failure analysis*, vol. 19, no. 1, pp. 13–21.
600 <https://doi.org/10.1016/j.engfailanal.2011.09.002>.

601 Christel, H., 2006. Aluminum Building Wire Installation and Terminations. *IAEI NEWS*, pp.
602 78–85.

603 <https://aluminum.org/sites/default/files/Aluminum%20Building%20Wire%20Installation>
604 [%20&%20Terminations.pdf](https://aluminum.org/sites/default/files/Aluminum%20Building%20Wire%20Installation%20&%20Terminations.pdf) (accessed: Jun. 06, 2021)

605 CM Group, 2020. An Initial Assessment of the Impact of the Covid-19 Pandemic on Global
606 Aluminium Demand. IAI. [https://www.world-](https://www.world-aluminium.org/media/filer_public/2020/05/28/initial_assessment_of_the_impact_of_the_covid-19_on_global_al_demand_.pdf)
607 [aluminium.org/media/filer_public/2020/05/28/initial_assessment_of_the_impact_of_the_](https://www.world-aluminium.org/media/filer_public/2020/05/28/initial_assessment_of_the_impact_of_the_covid-19_on_global_al_demand_.pdf)
608 [covid-19_on_global_al_demand_.pdf](https://www.world-aluminium.org/media/filer_public/2020/05/28/initial_assessment_of_the_impact_of_the_covid-19_on_global_al_demand_.pdf) (accessed: Apr. 28, 2021)

609 Cullen, J.M., Allwood, J.M., 2013. Mapping the Global Flow of Aluminum: From Liquid
610 Aluminum to End-Use Goods. *Environmental science & technology*, vol. 47, no. 7, pp.
611 3057–3064. <https://doi.org/10.1021/es304256s>.

612 Dai, M., Wang, P., Chen, W., Liu, G., 2019. Scenario analysis of China's aluminum cycle
613 reveals the coming scrap age and the end of primary aluminum boom. *Journal of Cleaner*
614 *Production*, vol 226, pp. 793-804. <https://doi.org/10.1016/j.jclepro.2019.04.029>.

615 Das, S.K., Green, J.A.S., Kaufman, J.G., Emadi, D., Mahfoud, M., 2010. Aluminum
616 recycling—An integrated, industrywide approach. *JOM*, vol. 62, no. 2, pp. 23–26.
617 <https://doi.org/10.1007/s11837-010-0026-6>.

618 Djukanovic, G., 2016. Aluminium alloys in shipbuilding – a fast growing trend. *Aluminium*
619 *Insider*. [https://aluminiuminsider.com/aluminium-alloys-in-shipbuilding-a-fast-growing-](https://aluminiuminsider.com/aluminium-alloys-in-shipbuilding-a-fast-growing-trend/)
620 [trend/](https://aluminiuminsider.com/aluminium-alloys-in-shipbuilding-a-fast-growing-trend/) (accessed: Apr. 09, 2021)

621 Djukanovic, G., 2017. Aluminium use in the production of trains steams ahead. *Aluminium*
622 *Insider*. [https://aluminiuminsider.com/aluminium-use-production-trains-steams-](https://aluminiuminsider.com/aluminium-use-production-trains-steams-ahead/#:~:text=Made%20in%20China%20%E2%80%93%20the%20high,speed%20of%20380%20km%2Fhr)
623 [ahead/#:~:text=Made%20in%20China%20%E2%80%93%20the%20high,speed%20of%](https://aluminiuminsider.com/aluminium-use-production-trains-steams-ahead/#:~:text=Made%20in%20China%20%E2%80%93%20the%20high,speed%20of%20380%20km%2Fhr)
624 [20380%20km%2Fhr](https://aluminiuminsider.com/aluminium-use-production-trains-steams-ahead/#:~:text=Made%20in%20China%20%E2%80%93%20the%20high,speed%20of%20380%20km%2Fhr) (accessed: Apr. 09, 2021).

625 Ducker Worldwide, 2011. Aluminum in 2012 North American Light Vehicles. Ducker
626 Worldwide, Troy, Michigan, USA. <http://www.drivealuminum.org/wp->

627 content/uploads/2017/05/2012_Aluminum-in-2012-North-American-Light-Vehicles.pdf
628 (accessed: Apr. 09, 2021)

629 Ducker Worldwide, 2012. EAA Aluminium penetration in cars - Final Report. Ducker
630 Worldwide, Troy, Michigan, USA. [https://www.european-aluminium.eu/media/1308/eea-](https://www.european-aluminium.eu/media/1308/eea-aluminium-penetration-in-cars_final-report-public-version.pdf)
631 [aluminium-penetration-in-cars_final-report-public-version.pdf](https://www.european-aluminium.eu/media/1308/eea-aluminium-penetration-in-cars_final-report-public-version.pdf) (accessed: Apr. 09, 2021)

632 Ducker Worldwide, 2017. Aluminum content in North American light vehicles 2016 to 2028.
633 Ducker Worldwide, Troy, Michigan, USA. [http://www.drivealuminum.org/wp-](http://www.drivealuminum.org/wp-content/uploads/2017/10/Ducker-Public_FINAL.pdf)
634 [content/uploads/2017/10/Ducker-Public_FINAL.pdf](http://www.drivealuminum.org/wp-content/uploads/2017/10/Ducker-Public_FINAL.pdf) (accessed: Apr. 09, 2021)

635 Eggers, A., Peeters, J.R., Waignein, L., Noppe, B., Dewulf, W., Vanierschot M., 2019.
636 Development of a computational fluid dynamics model of an industrial scale dense
637 medium drum separator. *Engineering Applications of Computational Fluid Mechanics*,
638 vol. 13, no. 1, pp. 1001–1012. <https://doi.org/10.1080/19942060.2019.1663559>.

639 European Aluminium Association, 2013. Aluminium in Cars - Unlocking the light-weighting
640 potential. [https://european-aluminium.eu/media/1326/aluminium-in-cars-unlocking-the-](https://european-aluminium.eu/media/1326/aluminium-in-cars-unlocking-the-lightweighting-potential.pdf)
641 [lightweighting-potential.pdf](https://european-aluminium.eu/media/1326/aluminium-in-cars-unlocking-the-lightweighting-potential.pdf) (accessed: Apr. 07, 2021)

642 European Aluminium Association, 2015. *The Aluminium Automotive Manual*.
643 <https://www.european-aluminium.eu/resource-hub/aluminium-automotive-manual/>
644 (accessed: Apr. 09, 2021)

645 European Aluminium Association, 2019. *VISION 2050: European Aluminium’s Contribution*
646 *to the EU’s Mid-Century Low-Carbon Roadmap*. [https://www.european-](https://www.european-aluminium.eu/media/2552/sample_executive-summary-vision-2050_web_pages_20190408.pdf)
647 [aluminium.eu/media/2552/sample_executive-summary-vision-](https://www.european-aluminium.eu/media/2552/sample_executive-summary-vision-2050_web_pages_20190408.pdf)
648 [2050_web_pages_20190408.pdf](https://www.european-aluminium.eu/media/2552/sample_executive-summary-vision-2050_web_pages_20190408.pdf) (accessed: Apr. 07, 2021)

649 Fog, K., 2019. *Hydro Market Outlook*. Norsk Hydro.
650 [https://www.hydro.com/Document/Index?name=Market%20outlook%20by%20Senior%](https://www.hydro.com/Document/Index?name=Market%20outlook%20by%20Senior%20)

651 20Vice%20President%20and%20Head%20of%20Corporate%20Strategy%20%26%20A
652 nalysis%20Kathrine%20Fog&id=7873 (accessed: Apr. 07, 2021)

653 Hannula, J., Godinho, J.R.A., Llamas, A.A., Luukkanen, S., Reuter, M.A., 2020. Simulation-
654 Based Exergy and LCA Analysis of Aluminum Recycling: Linking Predictive Physical
655 Separation and Re-melting Process Models with Specific Alloy Production. *Journal of*
656 *Sustainable Metallurgy*, vol. 6, no. 1, pp. 174–189. [https://doi.org/10.1007/s40831-020-](https://doi.org/10.1007/s40831-020-00267-6)
657 [00267-6](https://doi.org/10.1007/s40831-020-00267-6).

658 Hatayama, H., Daigo, I., Matsuno, Y., Adachi, Y., 2008. Assessment of Recycling Potential
659 of Aluminium in Japan, the United States, Europe and China. *Nihon Kinzoku Gakkai shi*,
660 vol. 72, no. 10, pp. 812–818. <https://doi.org/10.2320/jinstmet.72.812>.

661 Hatayama, H., Daigo, I., Matsuno, Y., Adachi, Y., 2012. Evolution of aluminum recycling
662 initiated by the introduction of next-generation vehicles and scrap sorting technology.
663 *Resources, conservation and recycling*, vol. 66, pp. 8–14.
664 <https://doi.org/10.1016/j.resconrec.2012.06.006>.

665 Hatayama, H., Yamada, H., Daigo, I., Matsuno, Y., Adachi, Y., 2006. Dynamic Substance
666 Flow Analysis of Aluminum and Its Alloying Elements. *Nihon Kinzoku Gakkai shi*, vol.
667 70, no. 12, pp. 975–980. <https://doi.org/10.2320/jinstmet.70.975>.

668 Kinsey, B., Wu, X., 2011. *Tailor Welded Blanks for Advanced Manufacturing*, 1st ed.
669 Woodhead Publishing, 2011. [https://www.elsevier.com/books/tailor-welded-blanks-for-](https://www.elsevier.com/books/tailor-welded-blanks-for-advanced-manufacturing/kinsey/978-1-84569-704-4)
670 [advanced-manufacturing/kinsey/978-1-84569-704-4](https://www.elsevier.com/books/tailor-welded-blanks-for-advanced-manufacturing/kinsey/978-1-84569-704-4) (accessed: Apr. 09, 2021)

671 Lamifil, 2019. Specialty wires. [https://lamifil.be/wp-content/uploads/2016/04/04-10-2019-](https://lamifil.be/wp-content/uploads/2016/04/04-10-2019-specialities-brochure-lr.pdf)
672 [specialities-brochure-lr.pdf](https://lamifil.be/wp-content/uploads/2016/04/04-10-2019-specialities-brochure-lr.pdf) (accessed: Apr. 09, 2021)

673 Lamifil, 2020. Aluminium alloys - Lamifil. <https://lamifil.be/products/aluminium-alloys/>
674 (accessed: Apr. 09, 2020)

675 Lupton, R.C., 2017. *ricklupton/sankeyview: v1.1.7*. Cambridge, United Kingdom.
676 <https://github.com/ricklupton/floweaver> (accessed: Apr. 09, 2021)

677 Lupton, R.C., Allwood, J.M., 2017. Hybrid Sankey diagrams: Visual analysis of
678 multidimensional data for understanding resource use. *Resources, conservation and*
679 *recycling*, vol. 124, pp. 141–151. <https://doi.org/10.1016/j.resconrec.2017.05.002>.

680 MakeItFrom, 2020. Aluminum Alloys :: MakeItFrom.com.
681 <https://www.makeitfrom.com/material-group/Aluminum-Alloy> (accessed: Apr. 09,
682 2021).

683 Matweb, 2020. Aluminum 4043-H18.
684 [http://www.matweb.com/search/datasheet_print.aspx?matguid=2541bb0127b34c7294612](http://www.matweb.com/search/datasheet_print.aspx?matguid=2541bb0127b34c7294612c77393ead8c)
685 [c77393ead8c](http://www.matweb.com/search/datasheet_print.aspx?matguid=2541bb0127b34c7294612c77393ead8c) (accessed: Apr. 09, 2021)

686 Modaresi, R., Lovik, A.N., Müller, D.B., 2014. Component- and Alloy-Specific Modeling for
687 Evaluating Aluminum Recycling Strategies for Vehicles. *JOM*, vol. 66, no. 11, pp. 2262–
688 2271. <https://doi.org/10.1007/s11837-014-0900-8>.

689 Modaresi, R., Müller, D.B., 2012. The Role of Automobiles for the Future of Aluminum
690 Recycling. *Environmental science & technology*, vol. 46, no. 16, pp. 8587–8594.
691 <https://doi.org/10.1021/es300648w>.

692 Nakajima, K., Takeda, O., Miki, T., Matsubae, K., Nakamura, S., Nagasaka, T., 2010.
693 Thermodynamic Analysis of Contamination by Alloying Elements in Aluminum
694 Recycling. *Environmental science & technology*, vol. 44, no. 14, pp. 5594–5600.
695 <https://doi.org/10.1021/es9038769>.

696 NTNU, International Aluminium Institute, TruthStudio, Davies, J., 2020. Global Aluminium
697 Cycle. IAI. <https://alucycle.world-aluminium.org/public-access/#global> (accessed: Apr.
698 08, 2021)

699 Paraskevas, D., Kellens, K., Dewulf, W., Duflou, J.R., 2015. Environmental modelling of
700 aluminium recycling: a Life Cycle Assessment tool for sustainable metal management.
701 Journal of Cleaner Production, vol. 105, pp. 357–370.
702 <https://doi.org/10.1016/j.jclepro.2014.09.102>.

703 Peng, T., Ou, X., Yan, X., Wang, G., 2019. Life-cycle analysis of energy consumption and
704 GHG emissions of aluminium production in China. Energy Procedia, vol. 158, pp. 3937-
705 3943. <https://doi.org/10.1016/j.egypro.2019.01.849>.

706 Prasad, N.E., Wanhill, R.J.H., 2016. Aerospace Materials and Material Technologies:
707 Volume 1: Aerospace Materials. Singapore: Singapore: Springer Singapore Pte. Limited.
708 [https://link-springer-com.kuleuven.ezproxy.kuleuven.be/book/10.1007%2F978-981-10-](https://link-springer-com.kuleuven.ezproxy.kuleuven.be/book/10.1007%2F978-981-10-2134-3)
709 [2134-3](https://link-springer-com.kuleuven.ezproxy.kuleuven.be/book/10.1007%2F978-981-10-2134-3) (accessed: Apr. 09, 2021)

710 Saevarsdottir, G., Kvande, H., Welch, B.J., 2020. Aluminum Production in the Times of
711 Climate Change: The Global Challenge to Reduce the Carbon Footprint and Prevent
712 Carbon Leakage. JOM, vol. 72, no. 1, pp. 296–308. [https://doi.org/10.1007/s11837-019-](https://doi.org/10.1007/s11837-019-03918-6)
713 [03918-6](https://doi.org/10.1007/s11837-019-03918-6).

714 Salazar, K., McNutt, M.K., 2010. Minerals Yearbook - Metals and Minerals 2010, vol. 1.
715 Eatsern Region, Reston, Va., USA: Department of the interior. Bureau of mines.

716 Schlesinger, M.E., 2017. Aluminum Recycling, 2nd ed. CRC Press.
717 <https://www.routledge.com/Aluminum-Recycling/Schlesinger/p/book/9781138073043>
718 (accessed: Apr. 07, 2021)

719 Soo, V.K., Peeters, J., Paraskevas, D., Compston, P., Doolan, M., Duflou, J.R., 2018.
720 Sustainable aluminium recycling of end-of-life products: A joining techniques
721 perspective. Journal of Cleaner Production, vol. 178, pp. 119-132.
722 <https://doi.org/10.1016/j.jclepro.2017.12.235>.

723 Southwire, 2020. Products | Southwire Overhead Transmission.
724 <https://overheadtransmission.southwire.com/products/> (Accessed: Apr. 09, 2020)

725 The Aluminum Association, 1989. Aluminum Electrical Conductor Handbook, 3rd ed.
726 Washington, DC, USA: Aluminum Association.
727 <https://www.aluminum.org/sites/default/files/Aluminum%20Electrical%20Conductor%20Handbook.pdf> (accessed: Jun. 06, 2021)

728

729 The Economist, 2007. The price of virtue.
730 <https://www.economist.com/leaders/2007/06/07/the-price-of-virtue> (accessed: Apr. 07,
731 2021)

732 The World Bank, 2021. GDP growth (annual %) | Data.
733 <https://data.worldbank.org/indicator/ny.gdp.mktp.kd.zg> (accessed: Apr. 09, 2021).

734 Van Heusden, R., Morrison, H., Puleo M., 2020. Why addressing the aluminium industry's
735 carbon footprint is key to climate action, World Economic Forum.
736 [https://www.weforum.org/agenda/2020/11/the-aluminium-industry-s-carbon-footprint-is-
737 higher-than-most-consumers-expect-heres-what-we-must-do-next/](https://www.weforum.org/agenda/2020/11/the-aluminium-industry-s-carbon-footprint-is-higher-than-most-consumers-expect-heres-what-we-must-do-next/) (accessed: Apr. 07,
738 2021)

739 Zhu, Y., Cooper, D.R., 2019. An Optimal Reverse Material Supply Chain for U.S. Aluminum
740 Scrap. *Procedia CIRP*, vol. 80, pp. 677–682. <https://doi.org/10.1016/j.procir.2019.01.065>.

741 Zhu, Y., Chappuis, L.B., De Kleine, R., Kim, H.C., Wallington, T.,J., Luckey, G., Cooper,
742 D.R., 2021. The coming wave of aluminum sheet scrap from vehicle recycling in the United
743 States. *Resources, Conservation and Recycling*, vol. 164.
744 <https://doi.org/10.1016/j.resconrec.2020.105208>.